Comparative Study of the Release Kinetics of Osmotically Active Solutes from Hydrophobic Elastomeric Matrices Combined with the Characterization of the Depleted Matrices

Dimitrios N. Soulas, Merope Sanopoulou, Kyriaki G. Papadokostaki

Institute of Physical Chemistry, Demokritos National Center for Scientific Research, 15310 Aghia Paraskevi Attikis, Athens, Greece

Received 21 October 2008; accepted 21 January 2009
DOI 10.1002/app.30100
Published online 30 March 2009 in Wiley InterScience (www.interscience.wiley.com).

ABSTRACT: The release process of three osmotically active solutes with various solubilities in water (NaCl, $CsNO_3$, and CsCl) from silicone rubber matrices is presented. The kinetics of release for different initial loads of the salts were supplemented by measurements of the kinetics of concurrent water uptake. To gain insight on the relevant non-Fickian transport mechanisms, the morphology, the diffusion and sorption properties and the physicochemical state of water in the salt-depleted matrices were studied. In addition, both salt-loaded and salt-depleted matrices were characterized with respect to their mechanical properties. The combined information, derived from these techniques, supported the operation of a release mechanism carried out through the formation of microscopic cracks, interconnecting the permanently formed cavities inside the matrices. The results indicate that these microscopic cracks may have healed upon drying. © 2009 Wiley Periodicals, Inc. J Appl Polym Sci 113: 936–949, 2009

Key words: diffusion; drug delivery systems; films; silicones

INTRODUCTION

Silicone rubber (SR) elastomers [crosslinked polydimethylsiloxanes (PDMSs)], because of their attractive properties of biocompatibility, good mechanical properties, and chemical inertness, are known to be ideal materials for the sustained release, in an aqueous environment, of lipophilic drugs incorporated in matrix controlled release systems of various geometries.[1–5] In these cases, the release takes place by the diffusion of the drug through the polymeric phase of the matrices. On the other hand, the release of hydrophilic drugs from hydrophobic systems in general[6,7] and SR elastomers in particular[8] is the outcome of the osmotic gradient that occurs because of the dissolution of the solute.

Moreover, another well-known method for promoting the release of hydrophilic drugs and proteins or accelerating the release of lipophilic ones is the use of osmotically active excipients, which, by causing an osmotic influx of water inside the matrices, alleviate the restrictions that the polymer poses on the release of the drugs. The use of osmotically active excipients has been applied both to the release of proteins[9] and drugs[10–13] from SR elastomers and the release of proteins from other elastomeric systems.[14–17]

Because inorganic salts are a group of chemicals that can cause the osmotic influx of water in hydrophobic systems, their transport properties in SR systems have been studied. Examples include the works of Golomb et al.,[18] Sutinen et al.,[19] and Riggs et al.,[20] who studied the release of $K_2Cr_2O_7$, NaCl, and NH_4F, respectively, from SR systems along with the measurement of the concurrent water uptake, taking into account the particle sizes and the initial salt load.

Furthermore, Schirrer et al.[21] and Amsden and coworkers,[22–24] having extensively studied the role of osmotic excipients of various particle sizes and at various volume fractions, gave quantified results and proposed mechanisms concerning the relation between the osmotic pressures (Π's) that build up in salt-containing pores and the rupture properties of the hydrophobic polymeric matrices. More specifically, according to the aforementioned mechanisms, immediately after the matrices are immersed in water, the superficial and easily accessible particles are rapidly dissolved and released. As water is

Correspondence to: K. G. Papadokostaki (kpapadok@chem.demokritos.gr).

progressively imbibed inside the matrices, because of the osmotic action of the particles, it enters the particle-containing cavities, and the particles are dissolved. The Π that builds up inside these cavities may be large enough to create microscopic cracks around them. These microscopic cracks progressively grow and percolate, creating small pathways.[20,21,24] Although in all of the studies the formation of microscopic cracks was a prerequisite, Amsden and coworkers[22,23] also proposed that the release kinetics of osmotically active excipients from monolithic matrices is also load dependent. Thus, if the initial volume fraction (v_N) of the excipients exceeds a certain percolation threshold, the particles may be either initially connected, or the surrounding polymeric walls, being of low thickness, are easy to rupture. In this case, the release may occur not only through the formation of microscopic cracks but also through the ruptured polymeric walls and has a significant effect on the observed release kinetics. Finally, in the case of moderately hydrophobic polymers (e.g., cellulose acetate), a third mechanism,[25] involving the formation of zones of enhanced hydration around the particle-containing cavities, was proposed to account for the observed release kinetics of highly soluble solutes from such polymers.

However, only a few data are available in literature concerning the remaining salt-depleted matrices and the changes that the polymer matrices undergo during the release of the osmotically active excipients in relation to the water uptake. Furthermore, because in all previous studies concerning SR, the used polymers were commercially obtained and, therefore, had various crosslinking procedures and chemical and physical properties, a direct comparison of the experimental data would be difficult.

The aim of this study was to make a comparative examination of

1. The release kinetics of three inorganic salts from SR matrices, with respect to their initial concentrations and differences in water solubility.
2. The variations on the kinetics and equilibrium of the concurrent water uptake.
3. The salt-depleted matrices with respect to their capacity for water uptake and mechanical properties and to compare these results with the corresponding data obtained for the salt-loaded matrices.

The results were supplemented by the thermal analysis of the swollen, salt-depleted matrices to gain insight into the state of the imbibed water and optical microscopy and scanning electron microscopy (SEM). Finally, the combined information, derived from the experimental data, is used to discuss the release mechanism in detail.

EXPERIMENTAL

Materials

Crosslinked PDMS (RTV 615 type) was kindly supplied by General Electric (Leverkusen, Germany). The silicone kit was a two-component system consisting of a vinyl-terminated prepolymer with high molecular weight (part A) and a crosslinker containing several hydride groups on shorter PDMS chains (part B). The curing of the PDMS membrane occurred via Pt-catalyzed hydrosilylation reaction to form a densely crosslinked polymer network.

The salts we used were NaCl (Riedel-de Haën Fine Chemicals, Hanover, Germany), $CsNO_3$ (Ventron Chemicals, Ltd., Karlsrue, Germany), and CsCl (Aldrich-Chemie, The Netherlands); all were analytical grade.

Salt particles (in the range 7–8 μm for NaCl and $CsNO_3$ and about 11 μm for CsCl) were obtained by the addition of acetone to stirred saturated aqueous solutions. The precipitate was dried and then ground in a vibrating mill (MKII, Grindex, Sweden) for about 24 h to dissociate aggregates formed upon drying. Finally, the retrieved salt particles were passed through a fine sieve to eliminate any remaining aggregates as much as possible. The particle sizes were evaluated by the means of optical and SEM microscopy of the loaded matrices.

Preparation of the matrices

Mixtures (10 : 1 w/w) of prepolymers parts A and B of SR were prepared by means of a mechanical stirrer at 400 rpm, degassed *in vacuo*, and then cast onto a polyethylene-coated plate by the means of a doctor's knife. Consequently, the cast films were cured at 100°C for 1 h according to the supplier's instructions to accelerate the crosslinking of the films. Additionally, for purposes of comparison, we obtained SR films with a higher degree of crosslinking (denoted henceforth as highly crosslinked) by mixing parts A and B at a 10 : 3 w/w ratio and following the aforementioned procedure.

We obtained the particle-loaded films (matrix thickness L = 380–420 μm) by dispersing the salt particles in the fluid SR mixture (10 : 1 w/w) before curing. To check the reproducibility of the results, two films corresponding to each concentration were prepared. The films contained NaCl in five different concentrations and $CsNO_3$ or CsCl in two. The initial load of each salt, expressed both as concentrations of grams of salt per 100 g of neat polymer and as v_N, is summarized in Table I, along with each salt's density and solubility in water at 25°C. Because the volume that the osmotically active agents occupied inside the matrices was one of the crucial factors that affected the release kinetics, the initial loads are expressed exclusively as v_N henceforth to allow the

TABLE I
Salt Densities, Solubilities in Water (at 25°C), Π's of Saturated Solutions, and Initial Salt Concentrations

Salt	Density (g/cm^3)	Solubility (mol/L)	Π (atm)	Initial salt concentration	
				% w/w[a]	v_N[b]
NaCl	2.17	6.10	346	3.9	0.02
				7.4	0.04
				15.7	0.07
				31.8	0.13
				62.4	0.23
$CsNO_3$	3.69	1.43	53	22.7	0.06
				51.3	0.12
CsCl	3.97	11.0	551	27.9	0.07
				62.2	0.14

[a] Grams of salt per 100 g of the neat polymer.
[b] Volume fraction (salt's volume per total matrix volume).

direct comparison of matrices of the same morphology regardless of the salts' densities.

The corresponding Π's; (Table I) of the saturated salt solutions at 25°C were calculated according to the following expression:[16]

$$\Pi = \frac{\Delta H_f \Delta T_f T}{V_l T_f T_f^*}$$

where ΔH_f is the latent heat of fusion of water (6012.2 J/mol),[26] ΔT_f is the freezing point depression of the corresponding saturated salt solution, T is the temperature of interest (298 K), V_l is the molar volume of water, T_f is the normal freezing point of water (273.15 K),[26] and T_f^* is the freezing point of the saturated solution, which was derived by the extrapolation of data acquired in the literature.[27]

Estimation of the degree of crosslinking of the neat and salt-loaded matrices

To estimate the degree of crosslinking of the neat and the salt-loaded films, samples were immersed in *n*-hexane[28] at room temperature and remained there until a constant weight was reached. Then, we estimated the degree of swelling ($q = 1 + V_{n\text{-hex}}/V_{SR}$, where $V_{n\text{-hex}}$ is the volume of the imbibed *n*-hexane and V_{SR} is the polymer volume that corresponds to each matrix) by weighing the films inside stoppered bottles as a precautionary measure to avoid the evaporation of *n*-hexane. The relation of q and the mean molecular weight by number between two consecutive crosslinks (M_c) was approximated by the following expression derived from Flory–Rehner theory:[29]

$$q^{5/3} \cong (\upsilon \cdot M_c)\frac{(1/2 - \chi)}{V_s} \quad (1)$$

where υ is the specific polymer volume (0.98 cm^3/g for SR), χ is the Flory–Huggins parameter for the linear PDMS and solvent system ($\chi = 0.4$ for the linear PDMS[30]), and V_s is the molar volume of the solvent (132 cm^3/mol).

Because the degree of crosslinking has an effect on the glass-transition temperatures (T_g's) of polymers,[31] the aforementioned results were also combined with the measurements of the T_g values of the neat matrices. The results were obtained by means of a model 2920 modulated differential scanning calorimeter (TA Instruments, New Castle, DE), in which the samples were originally cooled at −150°C and then heated with a nonmodulated signal and a 5°C/min heating rate up to 20°C.

Salt-release and concurrent water-uptake experiments in the salt-loaded matrices

Samples, of 2 × 2 cm^2 lateral dimensions, were cut from each of the salt-loaded films and mounted on stirring rods rotating at 37 rpm in frequently renewed, known volumes of distilled water thermostated at 25 ±0.1°C. The amount of salt released was measured at suitable time t and at $t \to \infty$ ($Q_{N,t}$ and $Q_{N,\infty}$, respectively) by means of a conductivity meter (Consort, Belgium, model K911, cell constant = 1 cm^{-1}, conductivity reading accuracy = 0.5%). Furthermore, we monitored the corresponding variation of the water content of the films ($Q_{w,t}$ at time t and $Q_{w,\infty}$ at $t \to \infty$) by weighing the blotted films at suitable time intervals and by taking into account the amount of salt that was released. At the end of the release experiments, the films were dried and weighed to check the amounts of permanently trapped salt particles.

Determination of the NaCl partition coefficients (K_N's) and diffusion coefficients (D_N's) in the salt-depleted matrices

At least three dried, salt-depleted matrices were immersed into a 2% w/v NaCl solution for a time period of 30 days. During this period, the films were periodically removed from the solution, blotted, and weighed until they reached a constant weight. Then, they were blotted, rinsed with distilled water, and placed into a known volume of distilled water. The NaCl desorption kinetics were monitored by means of the conductivity meter. After NaCl desorption was concluded, the films were removed from water, blotted, weighed, and then dried again to obtain the weight of the dry polymer and compare it with the corresponding values obtained after the release experiments.

The D_N's of NaCl were obtained from the first linear part of plots of $Q_{N,t}/Q_{N,\infty}$ versus $t^{1/2}/L$ by the use of eq. (2):[32]

$$\frac{Q_{N,t}}{Q_{N,\infty}} = 4\left(\frac{D_N t}{\pi L^2}\right)^{1/2} \text{ for } 0 \le \frac{Q_{N,t}}{Q_{N,\infty}} \le 0.6 \quad (2)$$

where $t^{1/2}$ is the square root of time t.

The K_N's were calculated for each matrix as the ratios of the solute concentration per volume of hydrated matrix to the solute concentration in the equilibrating solution (i.e., 2% w/v in the studied case). The permeability coefficients (P_N's) were calculated as the products of the corresponding values of D_N and K_N. Finally, the intrinsic partition coefficients ($k_{s,N}$) were calculated as the ratios of the solute concentration per volume of imbibed water in each matrix at the stage of equilibration with the 2%w/v NaCl solution to the solute concentration in the equilibrating solution.

Water sorption experiments in the salt-depleted matrices

To estimate the water sorption kinetics in the salt-depleted matrices, the said dried matrices were immersed in distilled water at room temperature. Consequently, they were periodically removed from water, blotted, and weighed until a constant weight was reached. Because eq. (2) is also valid for sorption experiments, in analogy to the previous paragraph (with the proper adjustment of the indicator N, corresponding to NaCl, to w, now corresponding to water), the apparent diffusion coefficients of water (D_w's), in the depleted matrices were estimated from the first linear part of plots of $Q_{w,t}/Q_{w,\infty}$ versus $t^{1/2}/L$.

Characterization of the state of water in the hydrated, salt-depleted matrices

The hydrated, salt-depleted matrices were characterized by means of the modulated differential scanning calorimeter to determine the state of absorbed water inside the formed pores. Samples weighing 5–10 mg were cut from these hydrated matrices and placed inside aluminum pans. The samples were cooled at −50°C in an inert nitrogen atmosphere and then heated at a 5°C/min rate with a modulated signal of ±0.796°C every 60 s up to 20°C.

Determination of the mechanical properties of the salt-loaded and salt-depleted matrices

Specimens were cut from the neat films (of standard and high degrees of crosslinking) and from both the salt-loaded matrices and the dried, salt-depleted ones to test their mechanical properties and acquire comparative values of the tensile modulus of elasticity. The instrument used was a Tensilon UTM-II-20 (Toyo Baldwin Co., Ltd., Japan). Each specimen had lateral dimensions of 1 × 0.1 cm^2, and their L varied from 380 to 420 μm. Stress–strain (f=ε) tests were performed with a ε rate of 20 mm/min at room temperature and 70% relative humidity.

SEM and optical microscopy of the salt-loaded and salt-depleted matrices

The morphology of the SR membranes was evaluated in the cross sections of the films both for the salt-loaded and salt-depleted matrices by use of a scanning electron microscope (Leo 440 SEM, Leo, Germany) and an optical microscope (Pol U-Amplival, Jena, Germany) equipped with a camera. The samples that were photographed by SEM were previously platinum-plated.

RESULTS AND DISCUSSION

Estimation of the degree of crosslinking of the neat and salt-loaded matrices

The experimentally determined values of q of samples in n-hexane were used to calculate M_c on the basis of eq. (1). The results are shown in Table II, where values of M_c are normalized to the neat SR matrices of standard crosslinking ($M_{c,SR}$; i.e., obtained by the mixture of parts A and B at a 10 : 1 w/w ratio).

In the case of the neat SR samples, the results of Table II indicate that increasing the concentration of the part B prepolymer in the precuring mixture increased, as anticipated, the degree of crosslinking and was in line with other findings in the literature.[28]

For the salt-loaded SR samples with standard crosslinking degrees, Table II shows that for $v_N \leq 0.07$, the measured q was practically equal to that of the corresponding neat SR, and the calculated $M_c/M_{c,SR}$ ratio was close to unity, which indicated that the crosslinking reaction was not materially affected by the presence of the salt particles. On the other hand, when $v_N > 0.07$, the $M_c/M_{c,SR}$ ratio exceeded unity, which pointed to a lower crosslinking degree, although the mixing ratios of parts A and B were the same in all cases (i.e., 10 : 1 w/w). Although the increase of q, especially at higher loads, may have partially been due to the solvent filling any gaps between the polymer and the embedded salt particles, one must also bear in mind that increasing amounts of solid

TABLE II
Values of q in n-Hexane, Molecular Weight Ratio ($M_c/M_{c,SR}$), and T_g for Neat Matrices with Either Standard or High Degrees of Crosslinking and Matrices Containing NaCl or $CsNO_3$

Sample	v_N	q	$M_c/M_{c,SR}$	T_g (°C)
SR (standard crosslinking)	0.00	2.46 ± 0.03	1	−125
SR (high crosslinking)	0.00	1.89 ± 0.10	0.77 ± 0.17	−115
Standard SR with NaCl	0.04	2.49 ± 0.06	1.02 ± 0.00	−125
	0.07	2.54 ± 0.05	1.05 ± 0.01	−125
	0.12	2.97 ± 0.04	1.37 ± 0.01	−125
	0.22	3.23 ± 0.09	1.58 ± 0.03	−126
Standard SR with $CsNO_3$	0.06	2.64 ± 0.02	1.13 ± 0.00	−125
	0.12	3.02 ± 0.05	1.41 ± 0.00	−126

particles in a fluid increases the latter's viscosity. Hence, the salt particles in the prepared fluid mixture, especially at volume fractions above 0.07, could have also produced an increase in its viscosity to such an extent that affected the unhindered approach of the polymeric chains. This, in turn, limited the extent of the vinyl-to-(Si—H) reaction and ultimately led to a lower degree of crosslinking.

In line with these results were the T_g values. In particular, matrices with $v_N \leq 0.07$ exhibited T_g's practically equal to the T_g values of the neat SR samples, which verified a similar degree of crosslinking. However, when v_N exceeded 0.07, a small but not negligible decrease in T_g was consistent with the findings that these matrices had a lower degree of crosslinking (Table II). In the case of the highly crosslinked neat matrices, T_g was significantly higher, which verified that, on the one hand, the changes in the crosslinking degree were more substantial and, on the other hand, the observed trend of the aforementioned salt-loaded matrices was correct.

Salt-release and concurrent water-uptake experiments in the salt-loaded matrices

Representative plots of the fractional amount $Q_{N,t}/Q_{N,\infty}$ of NaCl released from the salt-loaded matrices with various amounts of salt versus time t are shown in Figure 1(a).

After an initial steep portion (most probably due to particles easily accessible by water) corresponding to 5–8% of the initial load, the release curves of Figure 1(a) exhibited linear portions, that is, periods of constant release rates (cf. similar observations in refs. 21,22, and 33), which were more extensive in curves corresponding to $v_N = 0.04$, 0.07, and 0.13, whereas the magnitude of the release rate increased markedly with the salt load. Furthermore, as shown in Figure 1(b), the concurrent variation of $Q_{w,t}$ (g of imbibed water/g of dry polymer) appeared to follow an initial steep rise to a maximum water uptake ($Q_{w,\max}$) value, which was reached earlier for matrices with higher initial loads and was followed by a decline to a final water uptake ($Q_{w,\text{final}}$) value in the salt-depleted films. The results of $Q_{N,\infty}$, $Q_{w,\max}$, and $Q_{w,\text{final}}$ are summarized in Table III, where mean values from at least three samples are given for each of the two films studied. The corresponding rates of salt release, determined for the stages of release following the initial steep portion, together with the rates of the concurrent water uptake, are presented in Table IV. Both salt release and water uptake exhibited progressively increasing rates with initial loads. Moreover, it is also evident, that a small amount of NaCl was permanently retained inside the films, which did not, however, have an effect on the kinetics or the reproducibility of the results (Table III).

When the release kinetics curves were replotted on a $t^{1/2}/L$ scale [Fig. 1(c)], distinct deviations from Fickian kinetics were observed in all cases in the form of an S shape; similar findings were reported by Amsden et al.[22] These deviations, as the initial load increased, progressively became more pronounced, which implied the acceleration of NaCl transport through the films attributable to an osmotically induced excess influx of water, which, in turn, led to the formation of microscopic cracks inside the matrices (see the following).

The osmotically induced $Q_{w,\max}$ and, at the end of the experiment, $Q_{w,\text{final}}$ may also be expressed in terms of the fractional volumes of imbibed water corresponding to a maximum and to the end of the release experiments ($v_{w,\max}$ and $v_{w,\text{final}}$, respectively; volume of water per total matrix volume) and in Figure 2 are depicted as plots against v_N (volume fraction of NaCl in the SR films). It appears that $v_{w,\text{final}}$ did not vary significantly for the films with the three lower NaCl concentrations, whereas it increased at the two higher concentrations. Also, $v_{w,\text{final}} \gg v_N$ in all cases, although neat SR imbibed an amount of water as low as 0.002v/v at a water activity (α_w) of 1.[34] On the other hand, $v_{w,\max}$ appeared to increase for the first four concentrations, something which was reversed at the highest load. This unique, compared to the rest of the studied cases, behavior was attributable to the high initial load of these matrices, which was close to or exceeded the percolation threshold. Hence, in this case, a significant number of particles were not isolated, which permitted the formation of a pore network and/or led to surrounding polymeric walls of low thickness, which were easy to rupture. Thus, because of the rapid salt's release, the osmotic action inside the films was quickly diminished, which led to the lower $Q_{w,\max}$. As a result, in the case of matrices with $v_N = 0.22$, the release was predominantly diffusion controlled,[22,23] as indicated by the extensive linear regime on the $t^{1/2}$ scale in Figure 1(c).

Furthermore, another interesting observation was that the presence of the salts in the precuring mixture hindered the crosslinking of the two prepolymers, which must be also taken under consideration in the interpretation of the release mechanisms. More specifically, in the case of the matrices containing NaCl at an initial load of 0.13 v/v (also the case where the highest $Q_{w,\max}$ was recorded), the salt's release kinetics were not significantly enhanced compared to the kinetics recorded for matrices with an initial concentration 0.07 v/v. With the consideration that rupture occurred once the Π inside a salt-containing pore exceeded the fracture toughness of the surrounding material and that the matrices with 0.13-v/v NaCl loads were found to be crosslinked at a lesser degree (Table II), it appeared that, in this case, the polymer

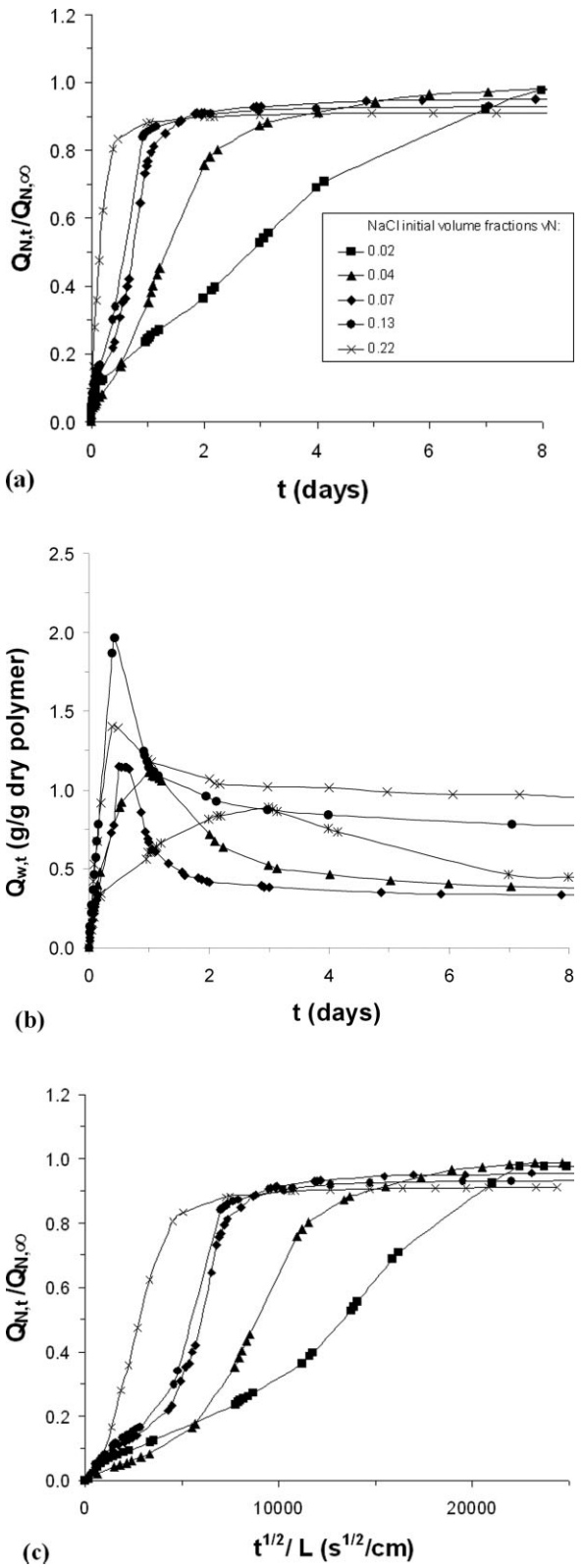

Figure 1 (a) Fractional NaCl release kinetic curves plotted on a t scale for v_N's of 0.02–0.23, (b) corresponding variations of osmotically induced water uptake during NaCl release, and (c) data from Figure 1a replotted on a normalized $t^{1/2}/L$ scale (L = 380–420 μm).

TABLE III
Results from the Salt-Release and Concurrent Water-Uptake Experiments in Salt-Loaded Matrices: Total Amount of Released Salt, Amount of Remaining Salt (Percentage of the Initial Salt Load), and $Q_{w,\max}$ and $Q_{w,\text{final}}$

Sample	v_N	$Q_{N,\infty}$ (g of salt/g of dry polymer)		Amount of remaining salt (%)		$Q_{w,\max}$ (g/g of dry polymer)		$Q_{w,\text{final}}$ (g/g of dry polymer)	
		1st film	2nd film	1st film	2nd film	1st film	2nd film	1st film	2nd film
Standard SR with NaCl	0.02	0.038 ± 0.002	0.039 ± 0.001	3.4 ± 1.2	2.7 ± 1.3	0.868 ± 0.041	0.932 ± 0.058	0.343 ± 0.041	0.463 ± 0.021
	0.04	0.073 ± 0.002	0.078 ± 0.001	8.0 ± 0.7	1.3 ± 0.0	1.082 ± 0.034	1.127 ± 0.103	0.402 ± 0.004	0.378 ± 0.012
	0.07	0.152 ± 0.004	0.140 ± 0.000	1.5 ± 0.5	7.1 ± 0.8	1.156 ± 0.025	1.050 ± 0.001	0.313 ± 0.021	0.431 ± 0.023
	0.12	0.293 ± 0.007	0.316 ± 0.007	3.0 ± 1.3	0.7 ± 0.2	1.967± 0.032	2.580 ± 0.010	0.724 ± 0.044	0.811 ± 0.011
	0.22	0.569 ± 0.005	0.575 ± 0.008	3.1 ± 0.9	1.0 ± 0.5	1.426 ± 0.073	1.104 ± 0.043	0.978 ± 0.079	0.805 ± 0.032
Standard SR with $CsNO_3$	0.06	0.190 ± 0.007	0.189 ± 0.020	14.7 ± 1.6	12.2 ± 3.9	1.730 ± 0.023	1.439 ± 0.112	1.096 ± 0.042	1.060 ± 0.060
	0.12	0.495 ± 0.028	0.467 ± 0.007	2.3 ± 1.8	6.8 ± 2.1	1.903 ± 0.062	1.946 ± 0.030	1.471 ± 0.054	1.410 ± 0.027
Standard SR with CsCl	0.06	0.229 ± 0.011	0.258 ± 0.004	11.5 ± 3.5	7.5 ± 1.8	1.018 ± 0.044	0.800 ± 0.021	0.622 ± 0.031	0.518 ± 0.023
	0.14	0.616 ± 0.063	0.559 ± 0.015	3.4 ± 1.3	4.7 ± 1.7	1.185 ± 0.067	1.212 ± 0.023	0.851 ± 0.190	0.852 ± 0.025

TABLE IV
Results from the Salt-Release and Concurrent Water-Uptake Experiments in Salt-Loaded Matrices: Salt-Release and Concurrent Water-Uptake Rates

Sample	v_N	Salt-release rate (%/h)		Water-uptake rate (g/g of dry polymer/h)	
		1st film	2nd film	1st film	2nd film
Standard SR with NaCl	0.02	0.44 ± 0.04	0.50 ± 0.04	0.010 ± 0.002	0.013 ± 0.000
	0.04	1.32 ± 0.12	1.40 ± 0.12	0.043 ± 0.004	0.046 ± 0.006
	0.07	3.49 ± 0.08	3.41 ± 0.07	0.078 ± 0.004	0.064 ± 0.000
	0.12	3.53 ± 0.11	3.70 ± 0.08	0.195 ± 0.003	0.176 ± 0.003
	0.22	11.5 ± 0.30	14.5 ± 0.26	0.243 ± 0.002	0.250 ± 0.007
Standard SR with $CsNO_3$	0.06	0.82 ± 0.01	0.86 ± 0.04	0.018 ± 0.000	0.020 ± 0.001
	0.12	1.31 ± 0.04	1.46 ± 0.02	0.035 ± 0.004	0.041± 0.003
Standard SR with CsCl	0.06	0.40 ± 0.06	0.62 ± 0.07	0.020 ± 0.000	0.019 ± 0.000
	0.14	2.35 ± 0.18	2.42 ± 0.12	0.036 ± 0.004	0.046 ± 0.000

posed smaller resistance to the swelling caused by the osmotically imbibed water. Hence, more water may have been imbibed before microscopic cracks could be formed;[21] this thus explains why the release rate was not as fast as anticipated.

Similar observations were made for the films that contained $CsNO_3$ or CsCl with respect to the salt-release kinetics and water uptake [Fig. 3(a–d)]. More specifically, the release curves deviated from the Fickian kinetics, exhibiting accelerating release rates with increasing initial loads, whereas the water uptake after reaching $Q_{w,\max}$, ended up to $Q_{w,\text{final}}$.

On the other hand, apart from the aforementioned similarities, the two other salts presented significant differences. In the case of $CsNO_3$-loaded matrices, the water-uptake rates were the slowest recorded and $Q_{w,\text{final}}$ was significantly higher compared to the other cases for similar initial loads. The slow water-uptake rates were attributable to the low osmotic action of $CsNO_3$ (Table I). The enhanced values of $Q_{w,\text{final}}$ were possibly related to the finding that the $CsNO_3$-loaded matrices appeared to start deviating from the nominal degree of crosslinking even at $v_N = 0.06$ (Table II). This, in turn, as discussed previously for NaCl-loaded matrices at $v_N = 0.13$, led to a delayed rupture of the pores,[21,24] which explained the enhanced water uptake.

In the case of CsCl, because of the highly hydrophilic nature of the salt (Table I), the particles tended to aggregate, and their dispersion was not fine. This, in contrast to the other two salts, led to the immediate release of a portion corresponding to about 40% of the initial load. The remaining amount did not produce adequate swelling as in the cases of NaCl or $CsNO_3$. Therefore, although CsCl was the most hydrophilic salt among the three, the osmotic action that it produced, for the given initial concentration, was sufficiently lower, which resulted in lower release rates and $Q_{w,\max}$ values.

Finally, as previously mentioned, in all cases, an amount of the initial load was permanently trapped inside the matrices. These amounts were totally secluded because the weights of the depleted, dried samples were the same even after they were equilibrated with NaCl, depleted, and then once again dried. The remaining amounts increased with the initial loads and were mainly observed in the cases of membranes containing $CsNO_3$ and CsCl. However, these amounts did not exceed 15% of the initial loads in any case. The presence of these remaining salt particles had an impact on $Q_{w,\text{final}}$. In the cases of matrices with $CsNO_3$ or CsCl, $Q_{w,\text{final}}$ appeared to increase compared to the cases of the NaCl-loaded films. Furthermore, the reproducibility of the water-uptake curves, in the late stages, was also affected by the presence of the remaining particles, although in all cases the release curves were reproducible. However, no overlapping between the water-uptake curves from membranes with different concentrations was noticed.

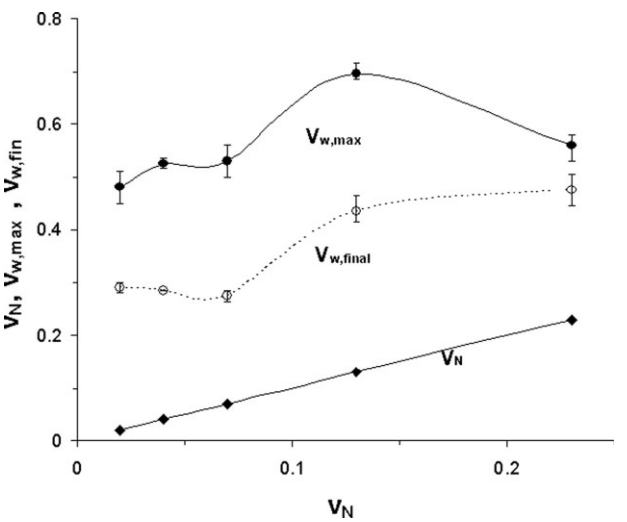

Figure 2 Variation in terms of the $v_{w,\max}$ (closed points) and $v_{w,\text{final}}$ (open points) values of osmotically induced water uptake plotted versus the salt load (v_N) for films initially containing NaCl.

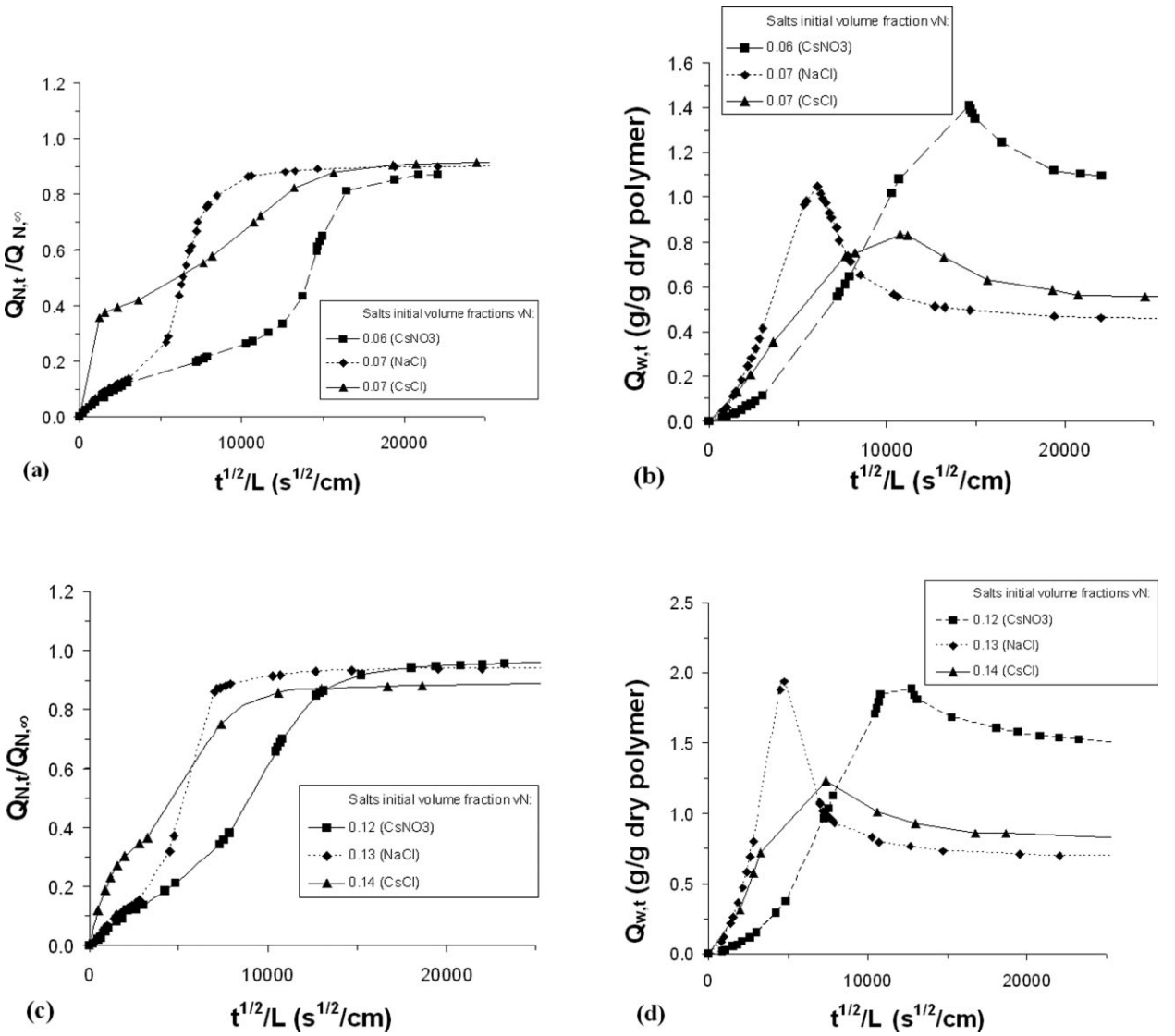

Figure 3 (a) Normalized salt-release kinetic curves on a $t^{1/2}/L$ scale for $v_N = 0.06$–0.07 and (b) corresponding variation of osmotically induced water uptake during salt release for $v_N = 0.06$–0.07. (c) Normalized salt-release kinetic curves on a $t^{1/2}/L$ scale for $v_N = 0.12$–0.14 and (d) corresponding variation of osmotically induced water uptake during salt release for $v_N = 0.12$–0.14 ($L = 380$–420 μm).

Determination of the mechanical properties of the salt-loaded and salt-depleted matrices

Typical stress–strain curves for two concentrations of NaCl-loaded matrices ($v_N = 0.07$ and 0.23) and the corresponding dried salt-depleted ones, along with that of neat SR, are shown in Figure 4(a), where f is the exercised stress and $\varepsilon = \Delta L/L_o$, where ΔL is the elongation and L_o is the initial sample length. The Young's modulus (E) was calculated from the slope of the first linear part of the aforementioned curves, and the results are reported in Table V. The Young's modulus for neat SR matrices (E_{SR}) was found to be 0.91 ± 0.02 MPa, which was in line with literature values (0.92 MPa,[34] $\sim$ 1 MPa[35]).

As shown in Table V, the presence of the salts increased E in all cases, whereas after their release, it was progressively reduced below the E_{SR} value corresponding to the neat SR matrix. In the cases of the $CsNO_3$- or CsCl-loaded matrices, E followed the same trend both for the salt-loaded and salt-depleted samples. It appeared, thus, that the said decrease depended solely on the volume that the salt particles left behind after their release and not on the different nature of the salts.

A way to predict the behavior of E in the salt-loaded matrices was to regard them as binary systems consisting of (1) a neat polymer continuum of E_{SR} (neat SR in our case) occupying volume fraction

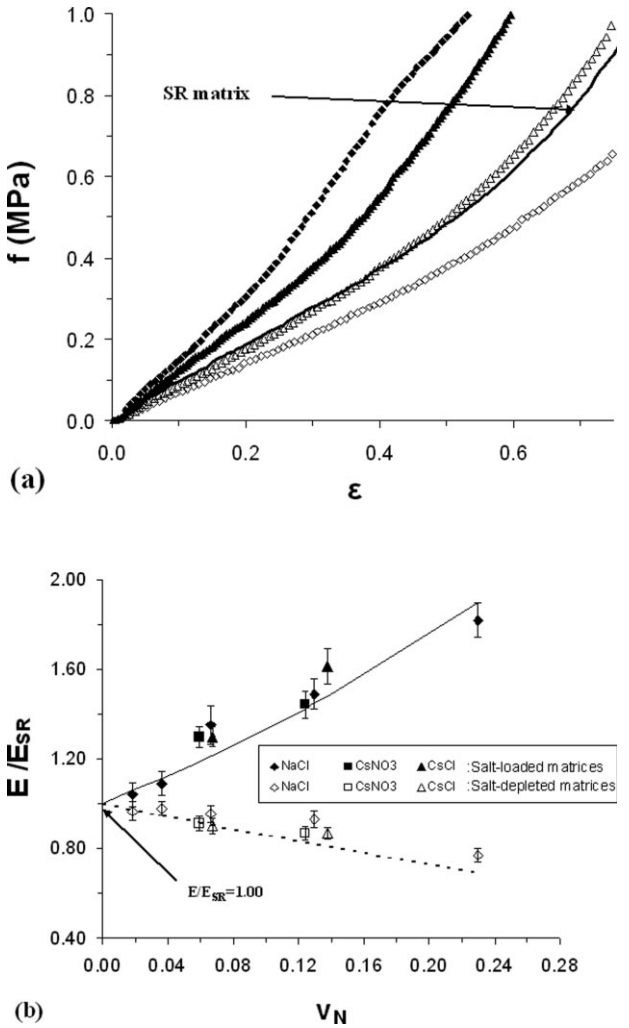

Figure 4 (a) Stress–strain curves for salt-loaded matrices (closed points) and corresponding salt-depleted matrices (open points) with NaCl at v_N values of (▲,△) 0.07 and (◆,◇) 0.23. (b) Experimental (points) and theoretical (lines) E/E_{SR} ratios for salt-loaded and salt-depleted matrices.

$v = 1 - v_N$ and (2) interspersed salt particles of v_N with an infinite Young's modulus (E_N). One then has to use the appropriate formula describing the dependence of E/E_{SR} from the volume fraction of the salt.[36] The formula introduced by Maxwell is

$$\frac{E}{E_{SR}} = 1 + 3v_N\left(\frac{a+2}{a-1} - v_N\right)^{-1} \quad (3)$$

where $a = E_N/E_{SR}$. For high values of E_N ($a \to \infty$), eq. (1) reduces to

$$\frac{E}{E_{SR}} = 1 + \frac{3v_N}{1 - v_N} \quad (4)$$

with regard to the salt-depleted matrices, we assumed that the volume fraction that was previously occupied by the salt particles was now occupied by air, which had an insignificant E compared to SR. Therefore, in this case, E_N, which now corresponded to the E of air, was practically zero and, therefore, accordingly, $a \to 0$. Thus, eq. (3) reduces to

$$\frac{E}{E_{SR}} = 1 - \frac{3v_N}{2 + v_N} \quad (5)$$

The lines shown in Figure 4(b) were calculated from eqs. (4) and (5) and were in good agreement with the experimental values of E/E_{SR} both for the salt-loaded and salt-depleted matrices. However, in the case of the NaCl-loaded matrices with $v_N = 0.22$, the small but distinct negative deviations from the theoretical curve may have been due to the smaller degree of crosslinking of these matrices compared to the neat SR matrices, as mentioned previously.

Furthermore, the decrease in E of the salt-depleted matrices, below the value of the neat SR matrix, implied the existence of permanent cavities after the depletion of the matrices consistent with the SEM micrographs (Fig. 5). The slightly positive deviations, apparent almost in all cases, may have partly been due to the remaining salt particles contributing to the rise in E and/or to the shrinkage of the pores upon drying.

Finally, the conformity of the experimental results for the salt-loaded matrices to eq. (4) indicated that the salt particles, with mean sizes in the range 7–11 μm, were finely dispersed in the polymer matrix in such a manner that, below the concentration of $v_N = 0.22$, their majority was isolated from one another, which thus allowed a large active surface.[37] In this way, strong interactions between the matrix and the particles were promoted, which ensured the contribution of the stiff filler to the E of the composite material. Composite materials containing particles of much higher sizes may not meet this criterion,

TABLE V
***E* Values of Neat Matrices with Standard or High Degrees of Crosslinking and of Salt-Loaded and Salt-Depleted Matrices**

			E (MPa)	
Sample	v_N	E_{SR} (MPa)	Loaded matrices	Depleted matrices
SR (standard crosslinking)	0.00	0.91 ± 0.02		
SR (high crosslinking)	0.00	2.10 ± 0.14		
Standard SR with NaCl	0.02		0.99 ± 0.04	0.92 ± 0.03
	0.04		1.03 ± 0.04	0.93 ± 0.01
	0.07		1.28 ± 0.07	0.91 ± 0.02
	0.12		1.41 ± 0.05	0.88 ± 0.02
	0.22		1.73 ± 0.05	0.73 ± 0.02
Standard SR with $CsNO_3$	0.06		1.23 ± 0.02	0.87 ± 0.01
	0.12		1.37 ± 0.04	0.82 ± 0.01
Standard SR with CsCl	0.06		1.23 ± 0.02	0.86 ± 0.02
	0.14		1.53 ± 0.06	0.82 ± 0.01

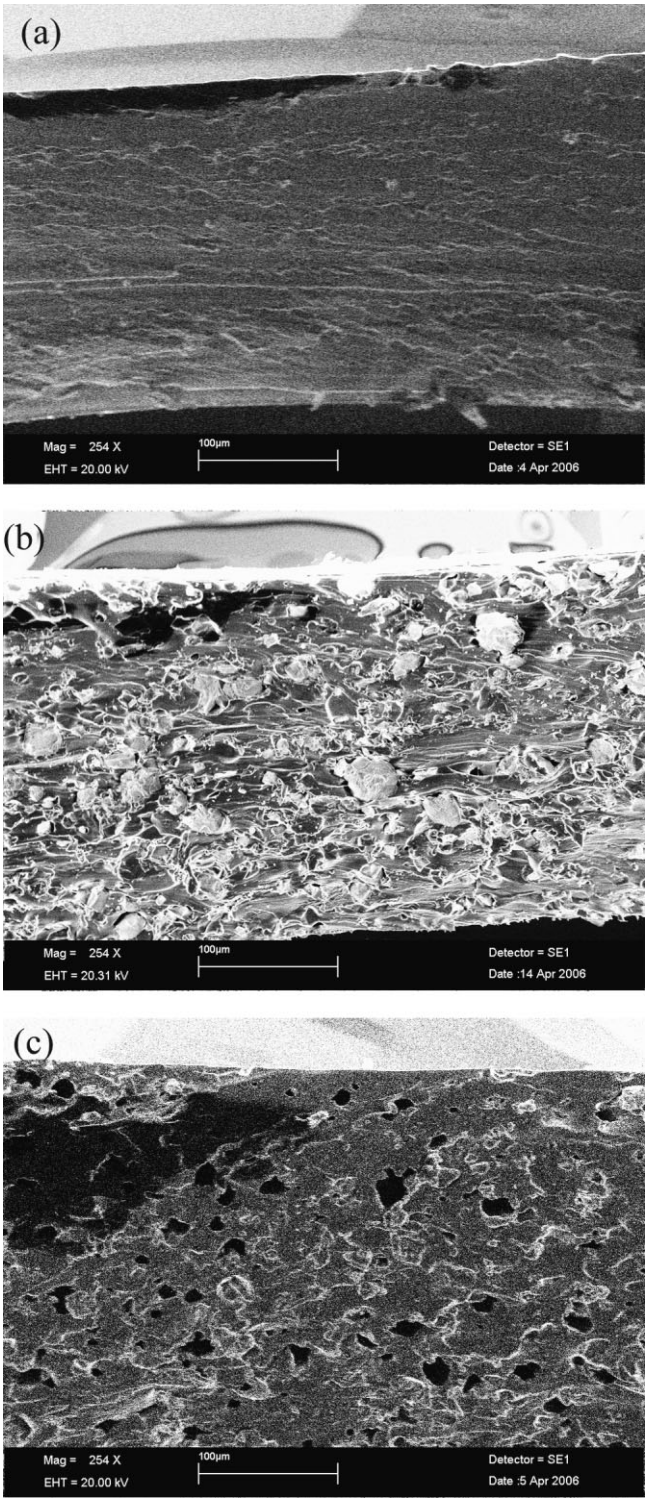

Figure 5 Representative SEM micrographs from the cross sections of (a) a neat SR matrix, (b) a matrix containing NaCl at $v_N = 0.13$, and (c) the previous matrix after the salt's release.

which would result in a decrease in E with increasing load, as, for example, in the work of Sutinen et al.,[19] where salt particles in the range 20–127 μm were used.

Characterization of the state of water in the hydrated solute-depleted matrices

The use of differential scanning calorimetry (DSC) at low temperatures provided the means to investigate the physicochemical state of water in the swollen matrices. The imbibed water inside a polymer matrix may be characterized as (1) freezable water that either appears to have a melting point ($T_{m,w}$) at 0°C and behaves, thus, as unbound (i.e., free water) or appears to have a $T_{m,w}$ below 0°C, which corresponds to water that occupies regions of small dimensions or interacts with the polymer itself, or (2) nonfreezable water, which because of its dispersion inside the polymer matrix or its interaction with the polymer does not freeze even when cooled below −100°C.[38] All of the DSC thermographs showed an endothermic peak because of the melting of the imbibed water in the salt-depleted matrices. The $T_{m,w}$ values are summarized in Table VI. In all cases, these $T_{m,w}$ values were below 0°C. This was due to, on the one hand, the fact that the water was sorbed into pores of small dimensions inside the matrices[39] and, on the other hand, the presence of the remaining salt, which contributed to the depression of $T_{m,w}$ below that of pure water.

The content of freezable water (Q_{wF}) inside the matrices, expressed in grams of water per grams of dry polymer, was calculated by the use of eq. (6):

$$Q_{wF} = \frac{\Delta H_m}{\Delta H_{mw}} \times \frac{m_{\text{sample}}}{m_{\text{dry polymer}}} \tag{6}$$

where ΔH_m is the heat absorbed during the melting of the water hydrating the matrices, which was estimated from the area of the endothermic peak; ΔH_{mw} is the melting enthalpy of free water (experimentally measured at 334.7 J/g, which was in good agreement with the literature value of 336.6 J/g[26]); m_{sample} is the hydrated sample mass; and $m_{\text{dry polymer}}$ is the mass of the corresponding dried sample.

We estimated the total content of water (Q_w) by weighing the hydrated samples and the corresponding dried ones. Consequently, the content of nonfreezable water (Q_{wNF}), was calculated as the difference between Q_w and Q_{wF}.

As shown in Figure 6, in all types of matrices, Q_{wF} increased linearly with Q_w. On the other hand, Q_{wNF} remained practically constant and equal to about 0.05 g of water/g of dry polymer (Fig. 6). Therefore, the excess content of water that was imbibed by each type of matrix behaved as free water. Because PDMS is a highly hydrophobic material, the presence of nonfreezable water may have been due to water confined in microscopic cracks. Moreover, the DSC results did not reveal any different behavior between matrices loaded with different salts, which suggested that the morphology of the corresponding

TABLE VI
$T_{m,w}$ (°C) of Water in Hydrated Salt-Depleted Matrices

Sample	v_N	$T_{m,w}$ (°C)
Standard SR with NaCl	0.02	−5.3 ± 0.1
	0.04	−5.5 ± 0.5
	0.07	−4.5 ± 0.5
	0.12	−3.8 ± 0.9
	0.22	−3.4 ± 0.2
Standard SR with $CsNO_3$	0.06	−3.0 ± 0.8
	0.12	−2.9 ± 0.4
Standard SR with CsCl	0.06	−5.2 ± 0.3
	0.14	−4.4 ± 0.5

salt-depleted matrices did not depend on the type of salt.

Determination of NaCl K_N's and D_N's in the salt-depleted matrices

The results of the sorption–desorption experiments are summarized in Table VII. The K_N's were found to be on the order of 10^{-3}, which, thus, showed that NaCl was excluded from the water-filled cavities of the matrices. The estimated $k_{s,N}$'s showed that the NaCl concentration in the sorbed water, inside the matrices, was 20–100 times smaller compared to the concentration in the equilibrating solution.

Furthermore, the water content of the matrices at equilibrium ($Q_{w,eq}$) with a 2% w/v NaCl solution, was significantly smaller compared to the values derived upon the equilibration of the depleted matrices with pure water (expressed as $v_{w,final}$ in Table VIII). This was because of differences in the α_w's between the equilibration solution ($\alpha_w = 0.989$) and pure water ($\alpha_w = 1.000$). Similar findings were also reported by Aschkenasy and Kost[7] when ethylene–vinyl acetate copolymer matrices containing NaCl were immersed in salt solutions and then immersed in distilled water. The corresponding $Q_{w,eq}$'s (Table VII) retained the same trend that was recorded after the release experiments, which, thus, showed that the permanently formed pores retained their relative sizes.

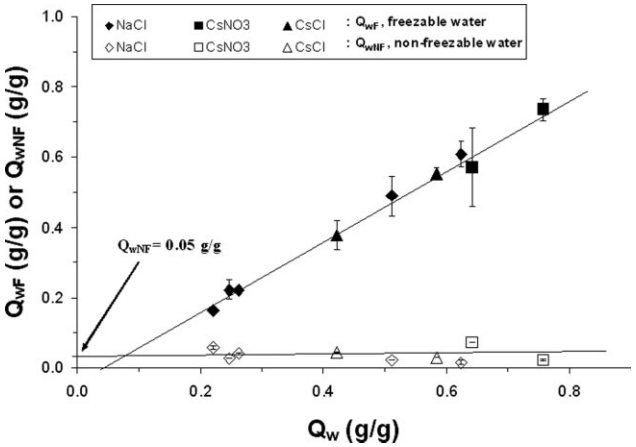

Figure 6 Q_{wF} (closed points) and Q_{wNF} (open points) for salt-depleted matrices initially containing NaCl, $CsNO_3$, and CsCl.

On the other hand, the D_N's of NaCl (Table VII), which were calculated from the first linear parts of the release curves plotted versus $t^{1/2}/L$ (examples shown in Fig. 7), were found to be two orders of magnitude higher than those calculated for particle-depleted films of cellulose acetate,[25] a moderately hydrophobic polymer (with a comparable Q_w), where NaCl could diffuse both through water-filled cavities and the hydrated polymeric phase. Therefore, the relatively high D_N values, which increased with increasing $Q_{w,eq}$, implied that the NaCl diffusion took place exclusively through interconnected water-filled cavities.

Water sorption experiments in the salt-depleted matrices

The kinetics of water uptake in representative salt-depleted matrices is shown in Figure 8. Assuming Fickian kinetics, we made an estimate of the D_w's with eq. (2), and they were found to be on the order of 10^{-10} cm^2/s (Table VIII). These values were smaller than those derived from the sorption

TABLE VII
Results from the Sorption–Desorption of NaCl Experiments in Salt-Depleted Matrices Initially Loaded at v_N

Sample	v_N	$Q_{N,eq}$ (10^{-5} g/g of dry polymer)	$Q_{w,eq}$ (g/g dry polymer)	K_N (10^{-3})	$k_{s,N}$ (10^{-2})	D_N (10^{-7} cm^2/s)	P_N (10^{-10} cm^2/s)
Standard SR with NaCl	0.02	2.4 ± 0.2	0.075 ± 0.000	1.1 ± 0.1	1.59 ± 0.11	1.0 ± 0.1	1.1 ± 0.1
	0.04	4.0 ± 0.5	0.126 ± 0.003	1.8 ± 0.2	1.57 ± 0.21	1.7 ± 0.1	2.9 ± 0.4
	0.07	4.3 ± 0.1	0.137 ± 0.006	1.9 ± 0.0	1.58 ± 0.09	2.6 ± 0.2	4.9 ± 0.2
	0.12	9.2 ± 0.5	0.171 ± 0.006	3.9 ± 0.2	2.71 ± 0.12	3.1 ± 0.1	12.3 ± 0.5
	0.22	17.1 ± 0.5	0.223 ± 0.016	7.0 ± 0.1	3.92 ± 0.21	4.0 ± 0.2	28.7 ± 1.4
Standard SR with $CsNO_3$	0.06	5.9 ± 0.2	0.307 ± 0.009	2.3 ± 0.1	0.97 ± 0.03	4.0 ± 0.3	7.0 ± 1.1
	0.12	11.4 ± 0.1	0.381 ± 0.012	4.1 ± 0.1	1.52 ± 0.05	4.8 ± 0.2	19.9 ± 0.8
Standard SR with CsCl	0.06	6.6 ± 0.2	0.200 ± 0.011	2.7 ± 0.1	1.67 ± 0.09	3.6 ± 0.1	9.8 ± 0.3
	0.14	11.1 ± 0.3	0.260 ± 0.013	4.4 ± 0.1	2.16 ± 0.10	4.0 ± 0.1	17.4 ± 0.5

$Q_{N,eq}$, Total amount of sorbed NaCl at equilibrium.

TABLE VIII
Results from the Water Sorption Experiments in Salt-Depleted Matrices Initially Loaded at v_N

Sample	v_N	$v_{w,final}$ (release experiments)	$v_{w,final}$ (water sorption)	D_w (10^{-10} cm^2/s)
Standard SR with NaCl	0.02	0.29	0.26	7.1
	0.04	0.27	0.25	5.9
	0.07	0.30	0.28	3.3
	0.12	0.44	0.42	1.9
	0.22	0.47	0.46	1.0
Standard SR with $CsNO_3$	0.06	0.50	0.49	2.5
	0.12	0.59	0.52	3.0
Standard SR with CsCl	0.06	0.38	0.37	5.7
	0.14	0.47	0.42	6.8

experiments of water vapor in neat SR[40–42] by four to five orders of magnitude. However, Barrie and Machin[43] found that, in the case of NaCl-doped SR, the water diffusivity decreased as much as 1000 times as silicone became saturated with water.

The water sorption experiments showed that the depleted matrices could sorb amounts of water slightly below the corresponding amounts at the end of the release experiments (Table VIII). If one takes into account that SR is a hydrophobic material, it is plausible to assume that the observed water sorption was provoked by the presence of the sustained salt particles. However, these amounts were not sufficient to justify exclusively the water sorption at such an extent, which led us to the conclusion that an intraconnected pore network existed in the depleted matrices, which was capable of accommodating the total amount of sorbed water. The low D_w values

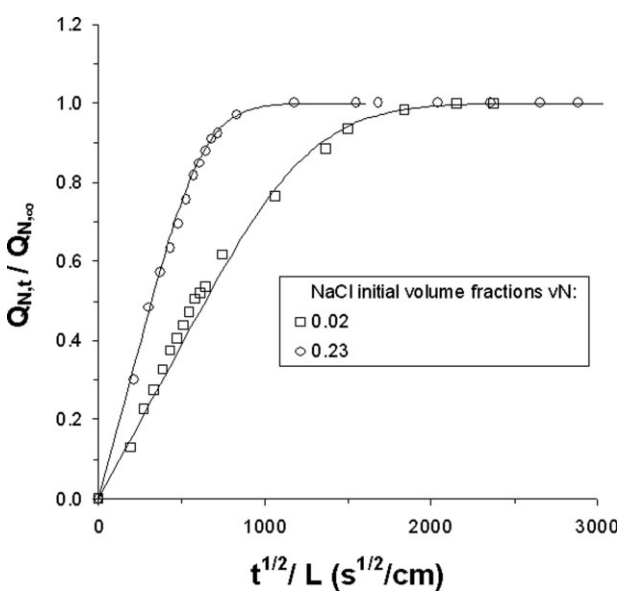

Figure 7 Kinetics of NaCl desorption (on a $t^{1/2}/L$ scale) from salt-depleted matrices equilibrated with an NaCl solution (2% w/v). The continuous lines correspond to Fickian kinetics.

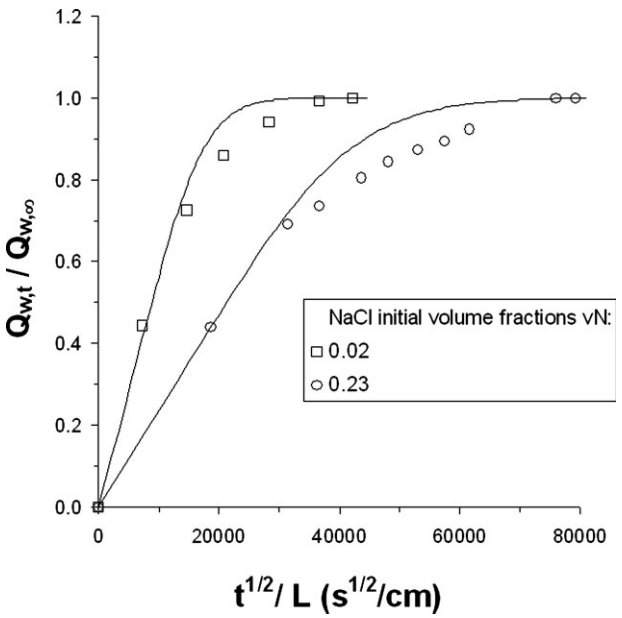

Figure 8 Kinetics of water sorption (on a $t^{1/2}/L$ scale) in salt-depleted matrices that initially contained NaCl. The continuous lines correspond to Fickian kinetics.

suggested that a secondary mechanism, possibly corresponding to the reopening of the pore network, took place during the water sorption by the depleted matrices.

Furthermore, this network, formed during the release experiments, could partially heal during the drying of the films because no evidence of its existence was supported by the mechanical properties of the salt-depleted matrices. However, a part of this healing was irreversible because the remaining amounts of water were, in all cases, slightly below the corresponding amounts recorded during the release experiments.

Discussion of the release mechanism

The overview of the release experiments of the three salts studied showed that

1. The rate of water uptake and the rate of salt released was enhanced with increasing v_N.
2. The water uptake reached a maximum during the release process, followed by a decline to $Q_{w,final}$, which exceeded the v_N that the salts originally occupied inside the matrix.
3. The release kinetics were strongly non-Fickian.

All of these findings were in line with the crack formation mechanism proposed by Schirrer et al.[21] on the basis of analogous results on similar SR–salt systems. According to this mechanism, as water is imbibed, the Π, created inside the salt-containing pores builds up and progressively may become large

enough to cause the creation of microscopic cracks, which grow and finally percolate, creating small pathways between the pores.

In this study, the examination of salt-depleted matrices provided further evidence in support of the said mechanism. In particular, although the estimated K_N's upon equilibration of the salt-depleted matrices with NaCl solutions were consistent with exclusion of the salt from the hydrophobic SR, nevertheless, the level of water sorption by far exceeded that of the neat SR polymer. This observation pointed to the existence of permanently formed cavities left behind by the depleted salt, capable of accommodating water upon equilibration of the matrices with salt solutions. In fact, the amount of imbibed water at the end of NaCl desorption from the fully hydrated, salt-depleted matrices increased with increasing v_N. The fact that the corresponding D_N values derived from these experiments increased with increasing amounts of imbibed water was consistent with salt diffusion through pathways connecting the water-filled cavities left by the salt. The practically constant amount of nonfreezable water determined by DSC in these matrices may have been due to water confined in regions of small dimensions, which would be either microscopic cavities or cracks in the fully hydrated, salt-depleted matrices.

A question that arose from the previous data is whether the permanently formed cavities created by the salt remained interconnected (through cracks) after the matrix was dried at the end of the release experiment or whether the microscopic cracks healed upon drying. The SEM micrographs of the dried, salt-depleted matrices showed permanently formed cavities but did not provide information on their possible interconnection. The elastic moduli of these types of matrices show close conformity to the theoretical predictions of a polymeric medium with dispersed air gaps of volume fraction equal to that of the initial salt load. Indications in favor of a healing upon drying crack mechanism were provided by the values of the estimated D_w derived from the pure water sorption experiments in dried, salt-depleted matrices, which, however, retained small amounts of salt (Table III). The latter were capable of inducing, to some extent, an osmotic influx of water (but could not fully account for the total amount of imbibed water, which was comparable to that at the end of the release experiments). The fact that the estimated apparent D_w values were approximately four to five orders of magnitude lower than those reported for neat SR[40–42] was possibly related to water transport, which was partly rate-determined by the slow reopening of microscopic cracks upon hydration.

However, a distinction must be made concerning the matrices with initial loadings equal or above 0.22 v/v. Because of the proximity of the particles, there was an increased probability of initially joined particles and of thin and easily ruptured cavity walls.[22] This led to the creation of sufficient pathways, in accordance to the cavity walls rupture mechanism, which enhanced the release kinetics of NaCl from these matrices. However, in this case, the formation of microscopic cracks was not discarded but considered as a supplementary mechanism.

Furthermore, the formation of zones of enhanced hydration around the particle-containing cavities[25] was not supported by the experimental data because there was no evidence that SR matrices could exceed their normal degree of hydration and accommodate the imbibed water elsewhere than either in the formed pores or in the microscopic cracks.

Although the aforementioned trends applied to all cases, regardless of the salts' solubilities in water and initial loads, and coincided with the results of previous works, certain deviations among the matrices loaded with different salts were also pointed out. Using a highly soluble salt such as CsCl as an excipient led to the rapid release of a significant amount of its initial load, which thus diminished the cumulative osmotic action inside the matrices. On the other hand, the use of a salt with moderate solubility in water, such as $CsNO_3$, led to a slow water uptake, which allowed the salt-containing pores to expand slowly. In addition, the lower crosslinking degree of these matrices led to delayed rupture and enhanced amounts of imbibed water. Finally, NaCl was an intermediate case with respect to both the water-uptake and salt-release rates.

CONCLUSIONS

A comparative study on the release kinetics from SR matrices of three salts with different solubilities in water was made. The combination of various experimental techniques allowed us to gain significant insight into the complex mechanisms operating during the release process of osmotically active solutes initially dispersed in highly hydrophobic polymeric matrices.

The overall picture that emerged through the study of the kinetics of salt release and concurrent water uptake in loaded matrices was in line with the formation of an interconnected network of cracks during the release process because of the osmotically enhanced ingress of water in salt-containing cavities. The extent of these phenomena depended on the solubility and the initial load of the salt. The morphology, mechanical properties, NaCl diffusion, and K_N's of the salt-depleted matrices confirmed the existence of permanently formed cavities left behind by the released salt particles. However, the low D_w in the salt-depleted matrices, which, as shown, contained

small retained amounts of salt, indicated that the microscopic cracks healed upon drying and reopened upon rehydration of the depleted matrices. At sufficiently high loads, a polymer wall rupture mechanism, operating in parallel to the microscopic crack formation mechanism, was possible.

References

1. Kydonieus, A. F. Controlled Release Technologies: Methods, Theory and Applications; CRC: Boca Raton, FL, 1980; Vol. 1, Chapter 2.
2. Ueno, N.; Refojo, M. F.; Liu, L. H. S. J Biomed Mater Res 1982, 16, 669.
3. Di Colo, G. Biomaterials 1992, 13, 850.
4. Schierholz, J. M. Biomaterials 1997, 18, 635.
5. Malcolm, R. K.; McCullagh, S. D.; Woolfson, A. D.; Gorman, S. P.; Jones, D. S.; Cuddy, J. J Controlled Release 2004, 97, 313.
6. Andreopoulos, A. G.; Plytaria, M. J Biomater Appl 1998, 12, 258.
7. Aschkenasy, C.; Kost, J. J Controlled Release 2005, 110, 58.
8. Amsden, B. J Pharm Pharm Sci 2007, 10, 129.
9. Carelli, V.; Di Colo, G.; Guerrini, C.; Nannipieri, E. Int J Pharm 1989, 50, 181.
10. Di Colo, G.; Carelli, V.; Nannippieri, E.; Serafini, M. F.; Vitale, D. Int J Pharm 1986, 30, 1.
11. Chetoni, P.; Di Colo, G.; Grandi, M.; Morelli, M.; Saettone, M. F.; Darougar, S. Eur J Pharm Biopharm 1998, 46, 125.
12. Woolfson, A. D.; Malcolm, R. K.; Morrow, R. J.; Toner, C. F.; McCullagh, S. D. Int J Pharm 2006, 325, 82.
13. Soulas, D.; Papadokostaki, K. G.; Sanopoulou, M. Desalination 2006, 200, 491.
14. Amsden, B.; Cheng, Y. L. J Controlled Release 1995, 33, 99.
15. Kajihara, M.; Sugie, T.; Hojo, T.; Maeda, H.; Sano, A.; Fujioka, K.; Sugawara, S.; Urabe, Y. J Controlled Release 2001, 73, 279.
16. Gu, F.; Younes, H. M.; El-Kadi, A. O. S.; Neufeld, R. J.; Amsden, B. G. J Controlled Release 2005, 102, 607.
17. Gu, F.; Neufeld, R.; Amsden, B. Pharm Res 2006, 23, 782.
18. Golomb, G.; Fischer, P.; Rahamin, E. J Controlled Release 1990, 12, 121.
19. Sutinen, R.; Bilbao-Revoredo, O.; Urtti, A.; Paronen, P. Int J Pharm 1989, 57, 155.
20. Riggs, P. D.; Kinchesh, P.; Braden, M.; Patel, M. P. Biomaterials 2001, 22, 419.
21. Schirrer, R.; Thepin, P.; Torres, G. J Mater Sci 1992, 27, 3424.
22. Amsden, B. G.; Cheng, Y. L.; Goosen, M. F. A. J Controlled Release 1994, 30, 45.
23. Amsden, B. G.; Cheng, Y. L. J Controlled Release 1994, 31, 21.
24. Amsden, B. G. J Controlled Release 2003, 93, 249.
25. Papadokostaki, K. G.; Amarantos, S. G.; Petropoulos, J. H. J Appl Polym Sci 1998, 69, 1275.
26. Lide, R. D. Handbook of Chemistry and Physics, 74th ed.; CRC: Boca Raton, FL, 1993.
27. International Critical Tables of Numerical Data: Physics, Chemistry and Technology; McGraw-Hill: New York, 1927; Vol. IV.
28. Stafie, N.; Stamatialis, D. F.; Wessling, M. Sep Purif Technol 2005, 45, 220.
29. Flory, P. J. Principles of Polymer Chemistry; Cornell University Press: London, 1953; Chapters 12 and 13.
30. Mark, J. E. Polymer Data Handbook; Oxford University Press: New York, 1999.
31. Gedde, U. W. Polymer Physics; Chapman & Hall: London, 1995; Chapter 5.
32. Crank, J. The Mathematics of Diffusion, 2nd ed.; Clarendon: Oxford, 1975.
33. Brown, D.; Bae, Y. H.; Kim, S. W. Macromolecules 1994, 27, 4952.
34. Nguyen, Q. T.; Bendjama, Z.; Clement, R.; Ping, Z. Phys Chem Chem Phys 1999, 1, 2761.
35. Van Krevelen, D. W. Properties of Polymers, 3rd ed.; Elsevier: New York, 1990.
36. Petropoulos, J. H. J Polym Sci Polym Phys Ed 1985, 23, 1309.
37. Frogley, M. D.; Ravich, D.; Wagner, H. D. Compos Sci Technol 2003, 63, 1647.
38. Ping, Z. H.; Nguyen, Q. T.; Chen, S. M.; Zhou, J. Q.; Ding, Y. D. Polymer 2001, 42, 8461.
39. Yamamoto, T.; Mukaib, S. R.; Nitta, K.; Tamonb, H.; Endoa, A.; Ohmoria, T.; Nakaiwa, M. Thermochim Acta 2005, 439, 74.
40. Watson, J. M.; Baron, M. G. J Membr Sci 1996, 110, 47.
41. Barrie, J. A.; Machin, D. J Macromol Sci Phys 1969, 3, 645.
42. Favre, E.; Schaetzel, P.; Nguyen, Q. T.; Clement, R.; Neel, J. J Membr Sci 1994, 92, 169.
43. Barrie, J. A.; Machin, D. J Macromol Sci Phys 1969, 3, 673.